

STUDY OF FRINGE FIELDS EFFECTS FROM FINAL FOCUS QUADRUPOLES ON BEAM BASED MEASURED QUANTITIES

T. Pugnat*, B. Dalena, CEA, Irfu, DACM, Université Paris-Saclay, F-91191, Gif-sur-Yvette, France
 A. Simona, L. Bonaventura, MOX, Politecnico di Milano, Milano, Italy
 R. De Maria, V.K. Berglyd Olsen, CERN, 1211 Geneva 23, Switzerland

Abstract

Accelerator physics needs advanced modeling and simulation techniques, in particular for beam stability studies. A deeper understanding of the effects of magnetic fields non-linearities will greatly help in the improvement of future colliders design and performance. In [1] and [2], a new tracking method was proposed to study the effect of the longitudinal dependency of the harmonics on the beam dynamics. In this paper, the study will focus on the effects on observable quantities in beam based measurements, for the case of HL-LHC Inner Triplet and with possible tests in LHC.

INTRODUCTION

In Ref. [1], a new tracking method was presented. It follows the work from Ref. [3] where the magnetic field map or the field harmonics are used to compute first a representation of the vector potential, which enters in the expression of the Hamiltonian, after the non-linear transfer map of the quadrupole is derived using Lie algebra techniques for tracking simulations. A strategy to interface the new map into SixTrack (Ref. [4]) without modifying its internal structure was presented, with some tests, in Ref. [2]. The choice of the integrator's order, z-step size and vector potential's gauge is made in order to optimize tracking accuracy and speed, see Ref. [5] for more details.

Using the new map and the longitudinal magnetic design of the prototype of the Inner Triplet (IT) for HL-LHC (see Fig. 1), this paper studies the impact of a more realistic description of the magnetic harmonic of IT quadrupoles on two observables: the Dynamic aperture (DA) and the amplitude detuning.

The HLLHC V1.0 optics with $\beta^*=15$ cm (Ref. [6]), and for one configuration (seed 1) of the machine with flat orbit, is used in all simulations unless otherwise specified. The novel method considers non-uniform multipoles distribution along the quadrupole. The IT heads (Fringe Fields) are modelled using 8 different vector potential files, according to the connector side and to the polarity (see Fig. 1), with only the natural harmonic of the quadrupole ($n=2,6,10,14$) for Lie2 ND0 and their derivatives up to order 6 for Lie2 ND6. The central part (body) of the quadrupoles are modelled using thin lenses with integrated multipole kicks, which are computed to keep the total integrated strength for each of the multipoles constant with respect to the other models.

This novel method is compared with uniformly distributed multipoles (called HE model) and uniformly distributed multipoles with additional multipole kicks at the quadrupoles'

extremities (called HE+heads model) as described in Ref. [7]. Random parts of field components (multipole kicks) are also considered in the body of the quadrupole. Finally, to ease the interpretation of the results in the two High Luminosity insertions, only the field errors of the IT are considered.

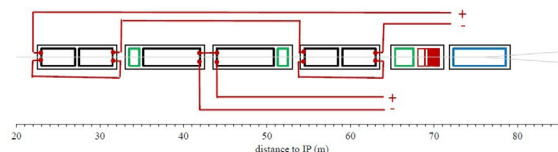
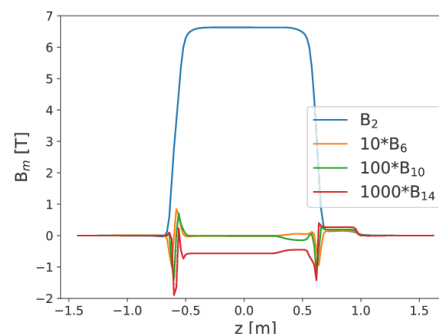


Figure 1: Normal harmonics sampled at $\Delta z = 2$ mm for the prototype of the IT quadrupole (top). IT powering scheme (bottom). Courtesy of E. Todesco and S. Izquierdo Bermudez

AMPLITUDE DETUNING

The amplitude detuning studies simulate the particles' motion over 10^3 revolutions purely on the vertical or horizontal plane, with and without the dodecapole correction (called MCTX). The initial positions are set to be below the DA value ($0 < 2J \leq 0.05 \mu\text{m}$, as shown in next section with a normalized emittance of $2.5 \mu\text{m}$), and their initial momentum offset δ is 0. As comparison, the maximum measured amplitude reached in the LHC is of the order of $0.3 \mu\text{m}$ for a β^* of 25 cm (see Ref. [8–10]).

In a preliminary study, a residual 1st-order detuning is observed in all the the models and planes. Part of it is removed by not considering the multipolar errors in the arcs and IR2-8. And when all b_4 multipole components are canceled, the remaining linear detuning is compatible with the 1st order anharmonicity given by MADX PTC (Ref. [11]) for the lattice without errors and with the main sextupole. Using a 4th order polynomial to fit tracking data, the linear coefficient C1 is about $1.8 \pm 0.1 \text{e-}2 \mu\text{m}^{-1}$ and $1.75 \pm 0.1 \text{e-}2 \mu\text{m}^{-1}$, in the x and y-planes respectively, and is subtracted from the following results. The choice of the polynomial's order for the fit is motivated by using smallest degree for the best score, and it's robustness over fitting procedures.

* thomas.pugnat@cea.fr

Figures 2 and 3 represent the detuning as a function of the initial amplitude for every model. The x-error bars correspond to the minimum and maximum amplitude over the 10^3 revolutions, and the y-error bars correspond to the uncertainty of the correction for linear detuning. The detuning from the tracking of each method is compared to the theoretical second order detuning component generated by the b_6 using the formula from Ref. [12]. They agree well up to an amplitude of $\sim 3.0 \times 10^{-2} \mu\text{m}$. It is worth noting that this second order is different according to the model, showing that amplitude detuning is an observable sensitive to the longitudinal distribution of the harmonics along the IT quadrupoles. In the horizontal plane and for amplitude higher than $\sim 3.0 \times 10^{-2} \mu\text{m}$, a deviation from the second order is visible, whose source is mostly due to the random component of higher order errors.

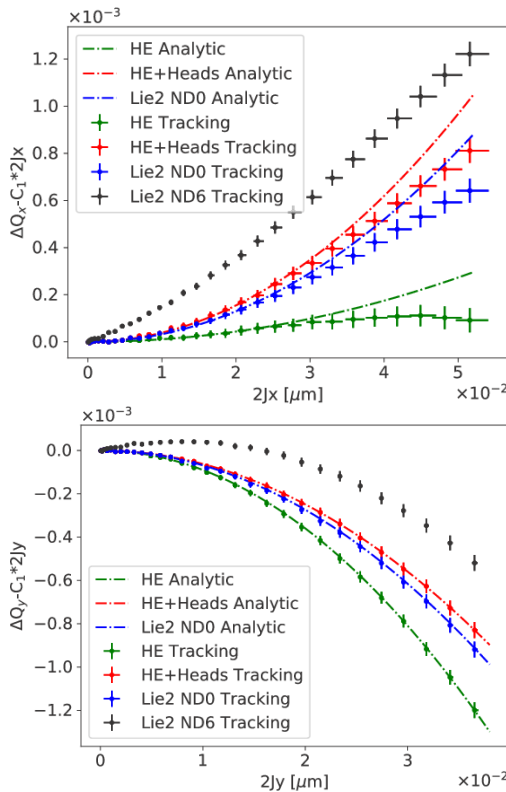


Figure 2: Amplitude detuning for the x-plane (top) and the y-plane (bottom). The b_6 corrector (called MCTX) has been switch OFF.

The comparison between the Lie2 models with and without derivatives (ND0 and ND6, respectively) show an additional linear detuning generated by the 1^{st} and 2^{nd} quadrupole derivatives, as expected from Theory. In a purely horizontal or vertical plane only the 2^{nd} derivatives contribute, but if we look at the coupling term, the contribution of both derivatives are equivalent. The 3^{rd} and 4^{th} derivatives can generate a 2^{nd} -order detuning. Nevertheless, for the Lie2 models, the 2^{nd} -order coefficient from the fit agrees well with a detuning purely due to the b_6 component, as can be seen from Table 1 where the 1^{st} and 2^{nd} order coefficient

of a polynomial fit to tracking data are shown. The linear detuning given by the derivatives (in the Lie2 ND6 model) is of the same order as the one given by the main sextupoles (C1) mentioned previously. The 2^{nd} coefficients are comparable to the theoretical values within their uncertainty for HE and HE with heads models. For the Lie2 models, the theory and the 2^{nd} order detuning are not comparable within the error, and part of discrepancy could be explained by the additional interpolation of the beta-function to have the values at each 2 cm.

Table 1: Amplitude Detuning from Fig. 2 fitted with a 4^{th} -order Polynomial. The Theoretical 2^{nd} -order coefficient is computed using the b_6 component only.

Case	$2\partial Q_x/\partial J_x$	$3\partial^2 Q_x/2!\partial J_x^2$	Theo. 2^{nd} order
HE	$(0.6 \pm 0.3)e^{-3}$	0.08 ± 0.03	0.11
HE+Heads	$(0.6 \pm 0.4)e^{-3}$	0.38 ± 0.03	0.39
Lie2 ND0	$(1.4 \pm 0.4)e^{-3}$	0.22 ± 0.03	0.32
Lie2 ND6	$(12.2 \pm 0.4)e^{-3}$	0.25 ± 0.03	0.32

Case	$2\partial Q_y/\partial J_y$	$3\partial^2 Q_y/2!\partial J_y^2$	Theo. 2^{nd} order
HE	$(0.2 \pm 0.4)e^{-3}$	-0.98 ± 0.05	-0.90
HE+Heads	$(-0.05 \pm 0.4)e^{-3}$	-0.62 ± 0.05	-0.62
Lie2 ND0	$(0.4 \pm 0.5)e^{-3}$	-0.79 ± 0.06	-0.68
Lie2 ND6	$(10.7 \pm 0.4)e^{-3}$	-0.67 ± 0.05	-0.68

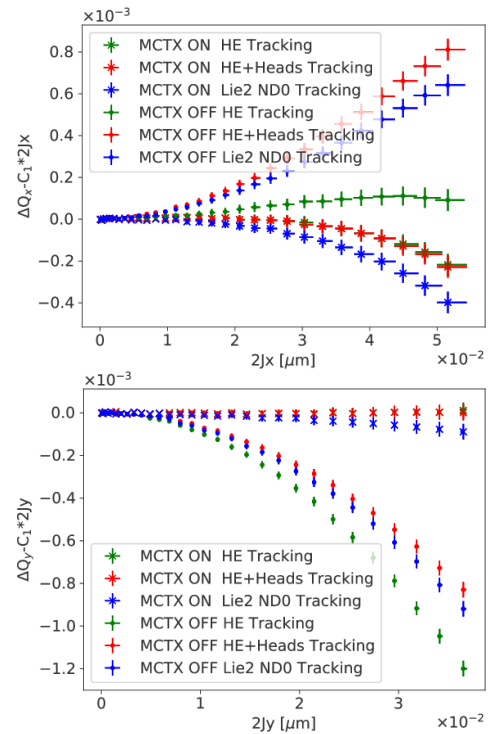


Figure 3: Comparison of amplitude detuning with and without correctors for the b_6 (MCTX).

Figure 3 shows the effect of the corrector for the b_6 , MCTX. In the case of the Lie2 models, its strength is equal

Content from this work may be used under the terms of the CC BY 3.0 licence (© 2019). Any distribution of this work must maintain attribution to the author(s), title of the work, publisher, and DOI

to the case HE with Heads. Since the case HE and HE with Heads seem to converge, the strength of MCTX appears to be correctly estimated in both cases. However, for Lie2 ND0, the correction is not enough in the vertical plane and too strong in the other.

DYNAMIC APERTURE

The DA is computed simulating the particles' motion over 10^4 revolutions with initial conditions distributed on a polar grid in such a way to have 30 particles (different initial conditions) for each interval of 2 sigma (beam size) from 0 to 28. Five phase space angles, according to field errors, are considered. The initial momentum offset δ is set to $27.e^{-5}$. The DA values are defined as losses occurred in 10^4 turns.

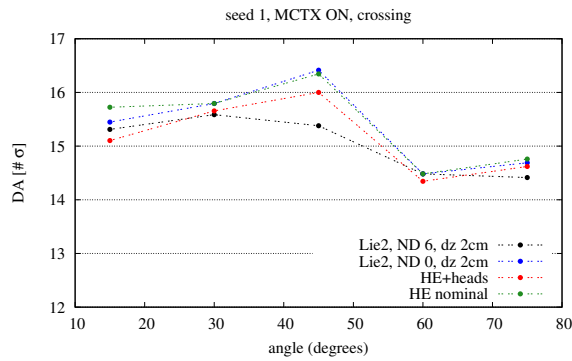


Figure 4: Dynamic aperture for a flat orbit optics, including the corrector for the b_6 (MCTX). The corresponding values for the HE and HE+heads models are shown for comparison.

Figure 4 shows the DA value considering the correction of the b_6 component of the IT (MCTX). The corrector calculation of the HE+heads case is used for the Lie2 model. The different models considered give the same DA within 1σ . In particular, the Lie 2 ND6 value at 45° shows the biggest difference with respect to the other models.

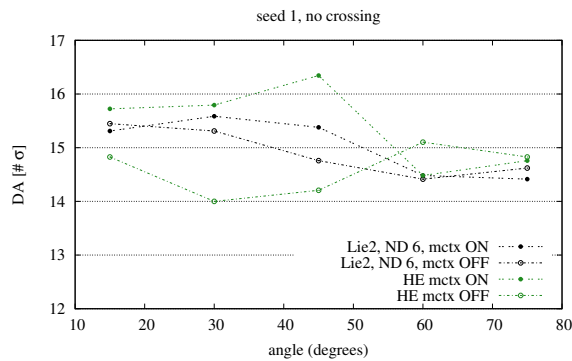


Figure 5: Dynamic aperture comparison with and without b_6 correction (MCTX) for the cases Lie2 ND6 and HE.

When the correction of the b_6 component of the IT is not considered, the DA value still shows the same one σ difference, with a maximum excursion at 30° , as shown in Fig. 5. The inclusion of the derivatives in the field heads is not necessary detrimental for DA though, and the lower DA

at 45° , when the b_6 correction is considered, seems to be due to the ineffectiveness of the correction, computed in the case HE+heads, for the case Lie2 ND6.

The minimum DA and the average DA values over 60 seeds are reported in Table 2 for each angle scanned in the tracking simulations. In particular, the minimum values are comparable for all the models within one σ , and the average values are equivalent between the different models (with a difference below 0.5σ , which is the DA calculation precision). The DA at 10^5 revolution has been calculated for the HE and the Lie2 ND6 models only. All the values are well within 0.5σ between the two models, i.e. converge to the same DA within its precision.

Table 2: Minimum and Average Computed DA Over 60 Seeds and 10^4 Turns, for Each Angle and Model Considered

Case	15°	30°	45°	60°	75°
minimum DA					
HE	14.8	15.0	15.5	13.8	13.9
HE+Heads	14.6	15.0	15.5	13.6	13.7
Lie2 ND0	14.7	15.0	15.6	13.4	13.7
Lie2 ND6	14.4	15.0	14.7	13.1	13.6
average DA					
HE	15.6	15.8	16.2	15.0	14.7
HE+Heads	15.5	15.6	16.2	14.7	14.5
Lie2 ND0	15.5	15.8	16.5	14.8	14.6
Lie2 ND6	15.4	15.6	16.1	14.5	14.3

CONCLUSION

The possibility to study Fringe Fields effects has been added to SixTrack code (Ref. [13]). The impact on beam based observables are studied in this paper, using tracking simulations of the HLLHCv1.0 optics.

The computation of DA as losses at 10^4 or 10^5 turns is not so sensitive to the longitudinal distribution of the field. The time evolution of the DA will be better investigated for the different models.

On the contrary, amplitude detuning is a good observable to see those effects. In this respect, beam based measurements on LHC show about 30% more linear amplitude detuning than expected by integrated magnetic measurements in the LHC (Ref. [10]). Since amplitude detuning is sensitive to Fringe Fields, it is planned to study their impact on the secondary lines of the frequency spectrum (RDTs) and on the coupling terms of the amplitude detuning.

The possibility to use β -beating or the phase advance as observables has also been attempted, using Machine Development data of 2016, 2017 and 2018 (Ref. [8–10]). No clear dependence with the amplitude has been observed so far.

ACKNOWLEDGEMENT

The authors would like to thanks S. Izquierdo-Bermudez and E. Todesco for providing the field harmonics computed

with ROXIE of the inner triplet prototype for the HL-LHC project and R. Tomas, E. H. Maclean, M. Giovannozzi and A. Chancé for useful discussions.

REFERENCES

- [1] B. Dalena *et al.*, “Fringe Fields Modeling for the High Luminosity LHC Large Aperture Quadrupoles”, in *Proc. IPAC'14*, Dresden, Germany, Jun. 2014, pp. 993–996. doi : 10.18429/JACoW-IPAC2014-TUPR0002
- [2] T. Pognat, B. Dalena, A. Simona, L. Bonaventura, R. De Maria, and J. Molson, “Accurate and Efficient Tracking in Electromagnetic Quadrupoles”, in *Proc. IPAC'18*, Vancouver, Canada, Apr.-May 2018, pp. 3207–3210. doi : 10.18429/JACoW-IPAC2018-THPAK004
- [3] M. Venturini and A. J. Dragt, “Accurate computation of transfer maps from magnetic field data”, *Nucl. Instr. Meth.*, vol. 427, pp. 387-392, May 1999.
- [4] SixTrack, <http://sixtrack.web.cern.ch/SixTrack>
- [5] A. Simona *et al.*, “High order time integrators for the simulation of charged particle motion in magnetic quadrupoles”, *Comp. Phys. Comm.*, vol. 239, pp. 33-52, February 2019.
- [6] R. De Maria *et al.*, “HLLHC V1.0: HL-LHC Layout and Optics Models for 150 mm Nb3Sn Triplets and Local Crab cavities”, in *Proc. IPAC'13*, Shanghai, China, May 2013, paper TUPFI014, pp. 1358–1360.
- [7] Y. Cai *et al.*, “Dynamic aperture studies for HL-LHC V1.0”, CERN-ACC-2018-0054.
- [8] E. H. Maclean *et al.*, “Report from LHC MDs 1391 and 1483: Tests of new methods for study of nonlinear errors in the LHC experimental insertions”, CERN, Geneva, Switzerland, Rep. CERN-ACC-Note-2018-0035, Jan. 2017.
- [9] E. H. Maclean *et al.*, “Report from LHC MD 2158:IR-nonlinear studies”, CERN, Geneva, Switzerland, Rep. CERN-ACC-2018-0021, Mar. 2018.
- [10] E. H. Maclean *et al.*, “Detailed review of the LHC optics commissioning for the nonlinear era”, CERN, Geneva, Switzerland, Rep. CERN-ACC-2019-0029, Feb. 2019.
- [11] MADX, <https://mad.web.cern.ch/mad>
- [12] A. W. Chao and M. Tigner, “Tune Dependence on Momentum and Betatron Amplitudes”, in *Handbook of Accelerator Physics and Engineering*, 2nd printing, 1999, pp. 73.
- [13] R. De Maria *et al.*, “SixTrack Version 5: Status and New Developments”, presented at IPAC'19, Melbourne, Australia, May 2019, paper WEPTS043, this conference.